Soft Matter

Active particles moving through disordered landscapes

Journal:	*Soft Matter*
Manuscript ID	SM-ART-10-2020-001942.R1
Article Type:	Paper
Date Submitted by the Author:	17-Dec-2020
Complete List of Authors:	Olsen, Kristian; University of Oslo, Department of Physics Angheluta, Luiza; University of Oslo, Department of Physics Flekkøy , Eirik; University of Oslo, Department of physics

Soft Matter

ARTICLE TYPE

Cite this: DOI: 00.0000/xxxxxxxxxx

Active Brownian particles moving through disordered landscapes

Kristian S. Olsen,*[a] Luiza Angheluta,[a‡] and Eirik G. Flekkøy[a]

Received Date
Accepted Date

DOI: 00.0000/xxxxxxxxxx

Disordered media are ubiquitous in systems where self-propelled particles are present, ranging from biological settings to synthetic systems, like in active microfluidic devices. Here we investigate the behavior of active Brownian particles that have an internal energy depot and move through a landscape with a quenched frictional disorder. We consider the cases of very fast internal relaxation processes and the limit of strong disorder. Analytical calculations of the mean-square displacement in the fast-relaxation approximation is shown to agree well with numerically integrated energy depot dynamics and predict normal dispersion for bounded drag coefficient and anomalous dispersion for power-law dependence of the drag on spatial coordinates. Furthermore, we show that in the strongly-disordered limit the self-propulsion speed can, for practical purposes, be considered a fluctuating quantity. Distributions of self-propulsion speeds are investigated numerically for different parameter choices.

1 Introduction

Transport of active matter in complex media has become a field of great importance and interest, not only because of its relevance to realistic biological systems, but also due to the possible new insights into non-equilibrium physics. In active matter systems a steady input of energy on the scale of the particles leads to self-propulsion, driving the system away from equilibrium [1,2]. Transport processes of biological entities typically take place in confining or disordered environments, leading to non-trivial behaviors. Examples include cell migration through the porous medium of the extracellular matrix [3], bacteria in soil [4], cells utilizing their environment to enhance transport [5], and various forms of *taxis*, like topotaxis [6,7] and curvotaxis [8], where cells direct their motion depending on substrate topography and curvature respectively. In such cases, it is insufficient to model the motion with an homogeneous active stochastic equation since the complex environment must be coupled to the particle motion. One way to do this is to also model the environment, for example as solid stationary obstacles [9], or even mobile or deformeable obstacles [10]. In a minimal approach à la homogenization theory, one can consider an effective model for the behavior on large scales where the particles experience spatially dependent drag, possibly leading to non-trivial dynamics. There are several instances imaginable where this could happen. For example, motion between two parallel plates with small local variations in the plate separation distance would lead to a local effective friction. One could also imagine a mean-field approach where one describes the dynamics of a single particle by including the effect of interactions with other particles through a spatially dependent friction that reflects the configuration of particles. Fig. (1) shows a third realization, where a simple setup allows for optical control of the viscosity, and hence drag, through a photorheological fluid [11].

In stochastic particle-based models of active matter, it is common to assume that the particles are self-propelled with a constant speed while the direction of motion changes stochastically, for example continuously in the case of active Brownian particles (ABPs) or discontinuously as in the case of run-and-tumble particles like e-coli [12,13]. However, this typically relies on an assumption that the dissipation due to drag is balanced by the kinetic energy production from the internal energy depot. In this paper we aim to elucidate the behavior of active particles in heterogeneous frictional landscapes, when such a balance is not necessarily achieved.

2 The depot model with heterogeneous friction

Different models of quenched spatial disorder have been considered in various ways, for example by random forces and potentials [14,15], inhomogenerous angular dynamics [16] and fixed hard obstacles [9]. However, not as much effort has been put into understanding soft spatial disorder like that of a complex frictional landscape. While the effect of viscosity gradients on the deterministic trajectories of squirmers has been studied [17], we here concern ourselves with minimal modeling of the stochastic dynamics of ABPs in the presence of various frictional landscapes.

To this end, we consider a version of the Schweitzer-Ebeling-Tilch energy depot model with a spatially inhomogeneous frictional force. This model for an ABP is classically expressed as the following set of evolution equations describing the stochastic particle dynamics coupled with a deterministic balance equation for

[a] *PoreLab, Department of Physics, University of Oslo, Blindern, 0316 Oslo, Norway*
‡ Present address: Kavli Institute for Theoretical Physics

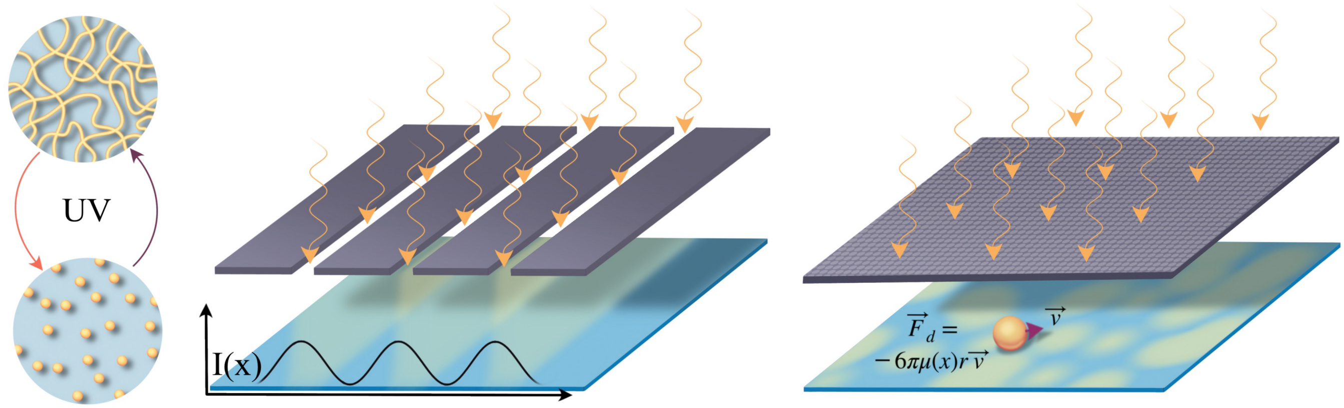

Fig. 1 Sketch of a setup where light can be used to control and design viscosity patterns in photorheological fluids. Such fluids typically have a polymeric suspension where the degree of entanglement in the polymeric network can be altered with UV light. Such setups can be used to optically control active or passive particles by strategically selecting appropriate optical filters, leading to a distribution of light intensities $I(x,y)$. Small spherical particles moving in such quasi-2D fluid environments experience a inhomogeneous Stokesian drag, as depicted in the rightmost figure.

the internal energy depot[18,19]:

$$\dot{x}_\alpha = v_\alpha \tag{1}$$

$$\dot{v}_\alpha = -[\gamma(x,y) - d_2\varepsilon(t)]\, v_\alpha + \sqrt{2D(x,y)}\xi_\alpha(t) \tag{2}$$

$$\dot{\varepsilon}(t) = q - c\varepsilon(t) - d_2u^2\varepsilon(t) \tag{3}$$

where α is the index of the spatial component and $u = |\vec{v}|$ is the self-propulsion speed (SPS). Here γ is the dissipative friction coefficient, and D is the noise amplitude, both being, in general, spatially heterogeneous in realistic disordered environments. In addition, particles can be accelerated at a rate dependent on their net internal energy ε and their speed v, with a proportionality coefficient d_2, here assumed a constant. In the passive limit $d_2 = 0$, we expect the Einstein relation to hold, leading to the spatial dependence also in the diffusivity. The restoring energy rate $q > 0$ is the rate at which the particle takes up energy from the environment and converts it into the internal energy depot ε, while c is the dissipation rate of the internal energy due to some various internal processes, like metabolism in the case of animals. Finally, ξ_α is the independent white noise, delta-correlated in time for each spatial component.

Throughout this article we will take the internal dissipation rate $c = 0$, which corresponds to the case where internal energy in only converted into motion. Most of the results presented here can be generalized to $c \neq 0$. We will also assume that fuel or nutrients are supplied homogeneously to the system, and we let q be a constant.

Some intuition for the above equations can be gained by considering the deterministic limit ($D = 0$) and calculating the energy dissipation rates. Let $K = u^2/2$ be the kinetic energy (mass is set to unity) and $E = K + \varepsilon$ the total energy of the particle. Then we have the equations

$$\dot{E} = q - \gamma(x,y)u^2 \tag{4}$$

$$\dot{K} = d_2\varepsilon u^2 - \gamma(x,y)u^2 \tag{5}$$

The particle increases its total energy with a rate q, and losses kinetic energy due to the environmental drag through the friction coefficient $\gamma(x,y)$. Furthermore, while kinetic energy is lost due to dissipation there is also a positive contribution $d_2\varepsilon u^2$ originating in the conversion of internal energy into kinetic energy.

2.1 Homogeneous case

Deterministic dynamics ($D = 0$): Before we generalize to a spatially-dependent friction coefficient, let us first consider what is known for the homogeneous case where $\gamma(x,y) = \gamma_0$ is a constant[12]. In this case, the general Eqs. (2)-(3) reduce to an equation for the self-propulsion speed $u(t)$ coupled to the internal energy depot $\varepsilon(t)$, namely

$$\dot{u}(t) = [-\gamma_0 + d_2\varepsilon(t)]u(t) \tag{6}$$

$$\dot{\varepsilon}(t) = q - d_2u^2\varepsilon(t) \tag{7}$$

This dynamical system has a non-trivial fixed point in the (u,ε)-phase space and given by $u_* = \sqrt{q/\gamma_0}$, $\varepsilon_* = \gamma_0/d_2$. To determine the stability of this fixed point, we linearize the dynamical system around its fixed point, i.e. $u = u_* + \delta u$, $\varepsilon = \varepsilon_* + \delta\varepsilon$, where the perturbations satisfy the linear equations

$$\frac{d}{dt}\begin{bmatrix}\delta u\\ \delta\varepsilon\end{bmatrix} = A\begin{bmatrix}\delta u\\ \delta\varepsilon\end{bmatrix} \tag{8}$$

where A is the Jacobi matrix associated to the nonlinear flow field and evaluated at the fixed point, and has components

$$A_{uu} = 0\,, A_{u\varepsilon} = d_2\sqrt{q/\gamma_0} \tag{9}$$

$$A_{\varepsilon u} = -2\sqrt{\gamma_0 q}\,, A_{\varepsilon\varepsilon} = -d_2q/\gamma_0 \tag{10}$$

The general solution of the linearized equations is given in terms of exponential functions $\exp(-t/\tau_\pm)$, where the relaxation time scale $\tau_\pm$ is the inverse of the eigenvalues of A. Using that $\mathrm{tr}(A) = -d_2q/\gamma_0$ and $\det(A) = 2d_2q$ and that both are invariant un-

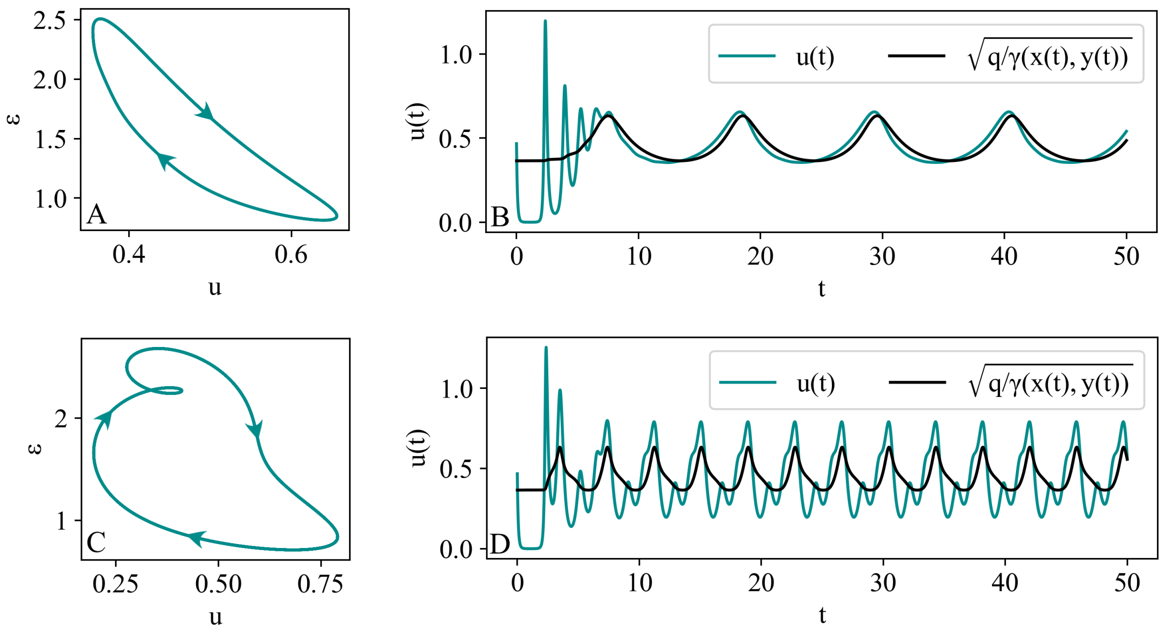

Fig. 2 Deterministic phase space dynamics and projected self-propulsion speed dynamics for a frictional landscape given by Eq. (19). Figures A,B show the case of a small wavenumber $k = 1$ ($\tau_I/\tau_S \approx 0.15$), displaying a good agreement with the naive extension of the homogeneous result $\sqrt{q/\gamma(\vec{x}(t))}$. Figures C,D show a case with $k = 3$ ($\tau_I/\tau_S \approx 0.45$), and we see that the two curves no longer match. Particles are initialized at $(x,y) = (0,0)$ with $(v_x, v_y) = (1/2, 0)$. Other parameters used are $\gamma_0 = 10, L = 5, q = 2, d_2 = 6$.

der diagonalization, one finds

$$\tau_{\pm}^{-1} = \frac{d_2 q}{2\gamma_0}\left[1 \pm \sqrt{1 - 8\frac{\gamma_0^2}{d_2 q}}\right] \tag{11}$$

Hence we may think of $\tau_I = \frac{2\gamma_0}{d_2 q}$ as the characteristic time scale for convergence to the stable fixed point.

Stochastic dynamics: The full stochastic dynamics drastically simplifies under the assumption that a stable fixed point has been reached. Using $v_x = u\cos\phi$ and $v_y = u\sin\phi$, with constant speed u, results in the following dynamics:

$$\dot{x}_\alpha = u\hat{P}_\alpha \tag{12}$$

$$\dot{\phi} = \sqrt{2D_\phi}\,\xi(t) \tag{13}$$

where $\hat{P} = (\cos\phi, \sin\phi)$ is the unit vector describing the particles direction of motion, and ξ is a scalar Gaussian white noise. We have also introduced $D_\phi = D/u^2$. This angular diffusivity sets the characteristic timescale for changing orientation $\tau_\phi = 1/D_\phi$.

The corresponding Fokker-Planck equation for the above equations take the form

$$\partial_t \Psi(x,y,\phi,t) + u\partial_\alpha[\hat{P}_\alpha \Psi(x,y,\phi,t)] = D_\phi \partial_\phi^2 \Psi(x,y,\phi,t) \tag{14}$$

where the second term is the self-advection due to the propulsion mechanism, and the term on the right-hand side is the angular diffusive term originating in the noise in the direction of motion. From the Fokker-Planck equation for the density Ψ one can derive equations of motion for expectation values through

$$\partial_t \langle f(\vec{x},\vec{v})\rangle = \int d\vec{x}\,d\phi\, f(\vec{x},\vec{v})\,\partial_t \Psi(\vec{x},\phi,t) \tag{15}$$

Using Eq. (14), one has the coupled equations

$$\partial_t \langle r^2\rangle = 2\langle u\hat{P}_\alpha x_\alpha\rangle \tag{16}$$

$$\partial_t \langle u\hat{P}_\alpha x_\alpha\rangle = u^2 - D_\phi \langle u\hat{P}_\alpha x_\alpha\rangle \tag{17}$$

This set of equations may be solved analytically for the mean square displacement, resulting in an effective late-time diffusion coefficient

$$D_{\text{eff}} \equiv \lim_{t\to\infty} \frac{1}{2}\partial_t \langle r^2\rangle = \frac{u^2}{D_\phi} \tag{18}$$

This implies a linear mean square displacement with $\langle r^2\rangle = 2D_{\text{eff}}t$. This well-known result for ABPs is in part what we want to generalize to active particles in heterogeneous frictional landscapes.

2.2 Heterogeneous case

In disordered media, the energy depot model (Eqs. (2)-(3)) does not simplify in a similar way to the homogeneous case. The simplest example of an heterogeneous medium is a regular and periodic landscape, such as those synthetically manufactured as sketched in Fig.(1). We consider a periodic system of size L with friction coefficient

$$\frac{\gamma(x,y)}{\gamma_0} = 1 + \frac{1}{2}\cos\left(k\frac{2\pi x}{L}\right)\cos\left(k\frac{2\pi y}{L}\right) \tag{19}$$

where k is the wavenumber. The characteristic length scale of this media is $\ell = L/k$. Averaged over the media, the mean speed of the particle is still $\sqrt{q/\gamma_0}$, and hence a characteristic time scale for motion through the medium can be set to $\tau_S = \ell\sqrt{\gamma_0/q}$. When

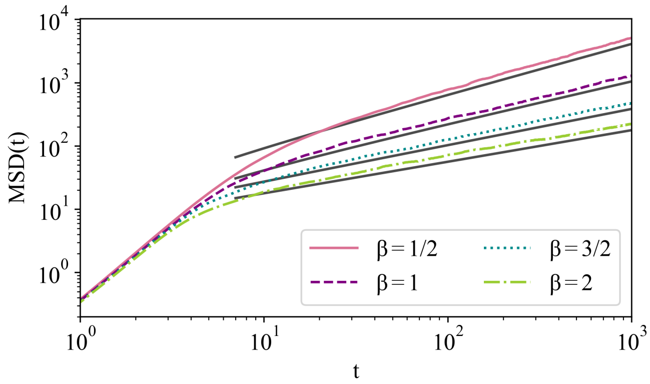

Fig. 3 Mean-square displacements (dashed colored lines) obtained by integrating the energy-depot equations Eq. (1) with $\gamma \sim r^{\beta}$, compared to the predicted scaling from the fast-relaxation model (solid black line). Parameters used: $d_2 = 1, q = 1/2, k_B T = 1, \gamma_0 = 0.1$. Ensemble averages are taken over 2000 particles.

compared to the time scale for internal relaxation τ_I we have

$$\frac{\tau_I}{\tau_S} = \frac{2}{\ell d_2}\sqrt{\frac{\gamma_0}{q}} \tag{20}$$

When τ_I is very small compared to τ_S the particle is able to adapt very quickly to the environment. In this limit one can expect that the system reaches the stable fixed point of the homogeneous deterministic system before the environment has had time to change considerably. We call this the fast relaxation approximation. In this regime the self-propulsion speed is well approximated by its fixed-point value $u(t) = \sqrt{q/\gamma(\vec{x}(t))}$. This limit is for example obtained if d_2 is very large, meaning that the particle is able to quickly convert internal energy into kinetic motion. τ_I is also small in the case where ℓ becomes large, or equivalently the wavenumber of the medium in Eq.(19) becomes small. Fig. (2) shows the phase space behavior for both small and larger wavenumber, showing how the particles dynamics. In upcoming sections we investigate the $\tau_I \ll \tau_S$ case separately, before considering a strongly disordered landscape where both short and long wavelength frictional modes are present.

3 Fast-relaxation approximation

We now consider the full stochastic dynamics associated with the fast relaxation approximation introduced above. The simple overdamped stochastic dynamics of Eq. (12) has been used with much success to model active Brownian particles in both trivial and non-trivial environments, like media with obstacles or scatterers. In the fast relaxation approximation, it makes sense to consider the Langevin description

$$\dot{x}_\alpha = u(x,y)\hat{P}_\alpha \tag{21}$$

$$\dot{\phi} = \sqrt{2D_\phi}\,\xi(t) \tag{22}$$

where $u(x,y) = \sqrt{q/\gamma(x,y)}$. Here we do not consider rotational drag or the effect of viscosity gradients on the length scale of the particle diameter, which may introduce additional torques which could be important for larger diameter particles.

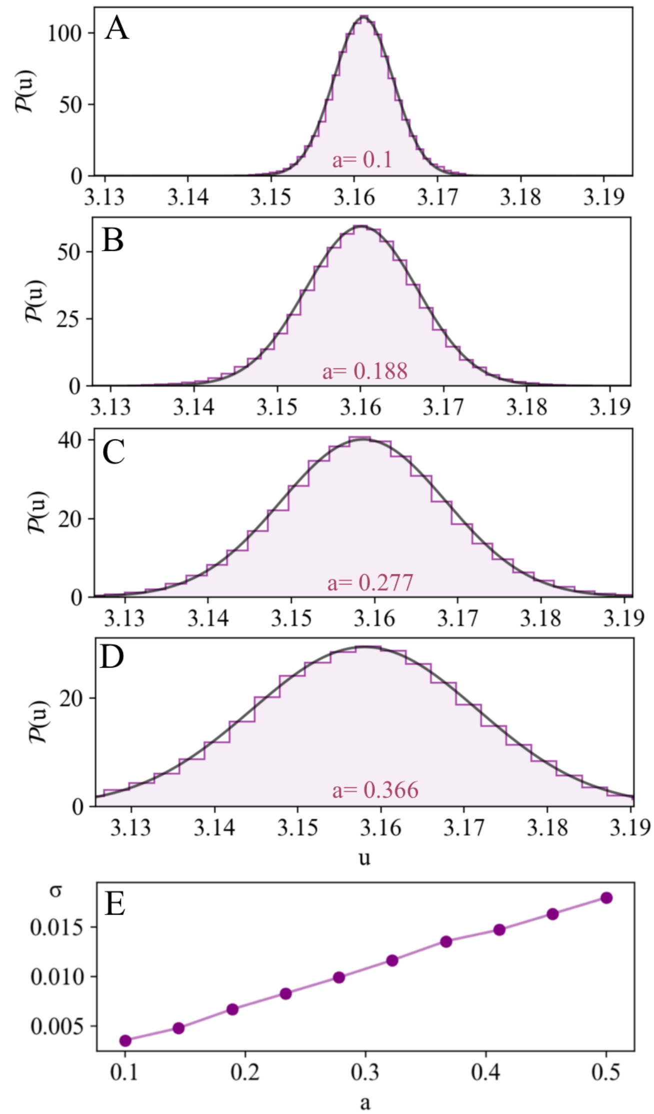

Fig. 4 Self-propulsion speed distribution obtained through averaging over random initial conditions in a quenched disordered landscape. Parameters used are $q = 2, \gamma_0 = 0.2, d_2 = 6$ with disorder strength amplitude a shown in the figure. Solid lines show Gaussian best fits. Note that the average value is close to $\sqrt{q/\gamma_0}$. Figure E shows the standard deviations as a function of disorder strength, displaying a linear relation.

The Langevin description in Eq.(21) has the Fokker-Planck equation

$$\partial_t \Psi + \partial_\alpha[u(\vec{x})\hat{P}_\alpha(\phi)\Psi] = D_\phi \partial_\phi^2 \Psi \tag{23}$$

A set of equations analogous to those in Eq. (16) can be obtained under the assumption of a slowly varying frictional landscape:

$$\partial_t\langle r^2\rangle = 2\langle u(\vec{x})\hat{P}_\alpha x_\alpha\rangle \tag{24}$$

$$\partial_t\langle u(\vec{x})\hat{P}_\alpha x_\alpha\rangle = \langle u^2(\vec{x})\rangle - D_\phi\langle u(\vec{x})\hat{P}_\alpha x_\alpha\rangle \tag{25}$$

In the case of homogeneous speed u the quadratic term above raises no problems, but here it may have a non-trivial temporal behavior. Multiplying Eq. (25) with $e^{D_\phi t}$ and using the inverse product rule one finds

$$\partial_t\left(\langle u(\vec{x})\hat{P}_\alpha x_\alpha\rangle e^{D_\phi t}\right)=\langle u^2(\vec{x})\rangle e^{D_\phi t} \tag{26}$$

Integration results in

$$\langle u(\vec{x})\hat{P}_\alpha x_\alpha\rangle = e^{-t/\tau_\phi}\int_0^t ds\langle u^2(\vec{x}(s))\rangle e^{s/\tau_\phi} \tag{27}$$

If the implicit time dependence of the u^2 factor is much slower than exponential we can extract the late-time behavior as

$$\langle u(\vec{x})\hat{P}_\alpha x_\alpha\rangle \sim \langle u^2(\vec{x})\rangle e^{-t/\tau_\phi}\int^t ds e^{s/\tau_\phi} \tag{28}$$

This results in $\langle u(\vec{x})\hat{P}_\alpha x_\alpha\rangle = \tau_\phi\langle u^2(\vec{x})\rangle$, which in turn implies for the mean square displacement that

$$\partial_t\langle r^2\rangle = 2\tau_\phi\left\langle\frac{q}{\gamma(\vec{x})}\right\rangle \tag{29}$$

Clearly the homogeneous result is re-obtained in the case of a constant SPS, while now there may be non-trivial temporal dependencies coming from $\langle u^2(\vec{x})\rangle$.

Various cases could now be considered. For example, in the case where the friction is a bounded function $\gamma_{\min}\leq\gamma(\vec{x})\leq\gamma_{\max}$ one can obtain bounds for the effective diffusivity rather trivially by inserting the bounds into the above equation. The unbounded case, however, is more interesting.

Consider a power-law medium $\gamma=\gamma_0 r^\beta$. This case has been much studied in the passive case, and has been used to model transport on fractals and other complex geometric structures[20–22]. Under the moment closure approximation $\langle r^{-\beta}\rangle = K\langle r^2\rangle^{-\beta/2}$, where K is some combinatorial factor that depends on the details of the closure scheme, one can integrate the equation for the mean square displacement, resulting in

$$\langle r^2\rangle \sim t^{\frac{2}{2+\beta}} \tag{30}$$

This is exactly the same anomalous diffusion behavior that is found for passive Brownian particles in similar viscosity landscapes[23]. At this point one should note that the prediction from this fast-relaxation model is not immediately clear from looking the full energy depot model in Eq. (2-3). The generalized friction term $\gamma(\vec{x})-d_2\varepsilon(t)$ may have a wide range of behaviors, since while the spatial friction grows in an unbounded way the internal energy storage also has no bounds in this model, and the particle will keep taking up energy leading to a diverging $\varepsilon(t)$ as well.

Fig. (3) shows the mean square displacement for an active particle with internal energy depot moving in a power-law medium $\gamma(x,y)\sim r^\beta$ with $\beta=1/2,1,3/2,2$. The fast-relaxation calculations predict a diffusion exponent of $2/(2+\beta)$, which in the figure are shown in solid lines.

4 Disordered frictional media

So far we have studied the fast-relaxation limit where the particles respond instantly to the surrounding medium. We now consider the opposite extreme, where a rapidly changing random medium causes the particle to change its dynamics before it has time to relax internally. We consider the deterministic dynamics again, as we did previously for a single wavelength viscosity, and focus on the randomness originating in a random medium rather than thermal noise.

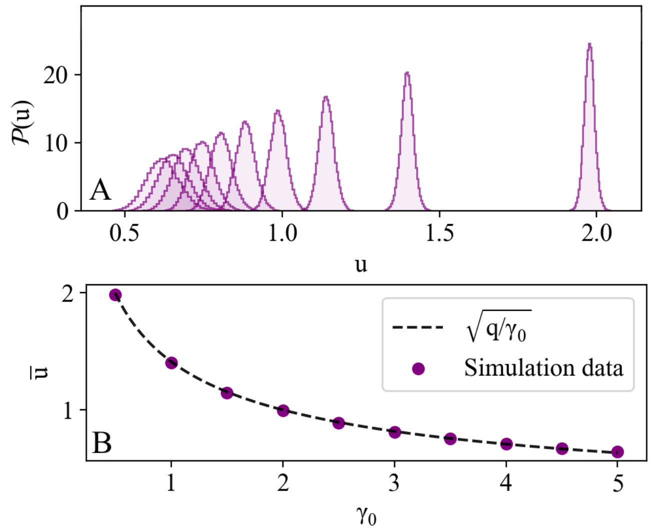

Fig. 5 A) Dependence of distributions on friction parameter γ_0.B) Mean value follows the curve $\sqrt{q/\gamma_0}=\sqrt{q/\langle\gamma\rangle}$. Parameters used: $q=2, d_2=6, a=0.5$.

To model a strongly disordered landscape, we consider a periodic system of length L and write the friction coefficient as a random Fourier series in the form

$$\frac{\gamma(x,y)}{\gamma_0}=1+aF(x,y), \tag{31}$$

$$F(x,y)=\sum_m\left[a_m\cos\left(\frac{k_m x}{L}\right)+b_m\sin\left(\frac{k_m x}{L}\right)\right] \times\left[c_m\cos\left(\frac{k'_m y}{L}\right)+d_m\sin\left(\frac{k'_m y}{L}\right)\right] \tag{32}$$

where $\{a_m,b_m,c_m,d_m\}$ are Gaussian random variables with zero mean and unit variance and $\{k_m,k'_m\}$ and integer uniform random variables. The dimensionless parameter $a\in(0,1)$ is the disorder strength.

In simulations, particles are initialized with random initial direction of motion with $(x,y)=(0,0)$. The energy depot equations Eq. (2-3) are integrated for 2000 particles and their self-propulsion speeds are sampled. In practice, the random wavenumbers together with L and the number of terms in the sum in Eq. (31) should be chosen as to avoid a sparse sampling of wavenumbers. Unless otherwise stated we use as a representative case $k_m,k'_m\in(0,50)$ with $L=5$ and 70 random terms. Results do not vary significantly with other representative choices of parameters.

In the disordered case where several random Fourier modes are present, the self-propulsion speed fluctuates. First, we consider the limit of weak disorder strength, where both a and the friction strength γ_0 are reasonably small. Fig. (4) shows the distribution of self-propulsion speeds obtained by running ensemble averages over different particle initial conditions of the same quenched disordered media generated by Eq. (31). The resulting normal distributions have a standard deviation that grows linearly with the disorder strength a, as shown in Fig. (4 E). Fig. (5) shows the dependence of the mean self-propulsion speed with friction strength γ_0, showing a clear $1/\sqrt{\gamma_0}$ dependence.

In the limit of strong friction ($\gamma_0 \gg 1$), the mean approaches zero and the Gaussian shape disappears and the probability distribution function becomes skewed. Fig. (6) shows self-propulsion speed distributions in this regime. The distributions in this regime can for certain parameter choices (eg. Fig. (6 B)) appear to have exponential tails, while for other choices (eg. Fig. (6 C)) the tail is neither exponential nor power-law.

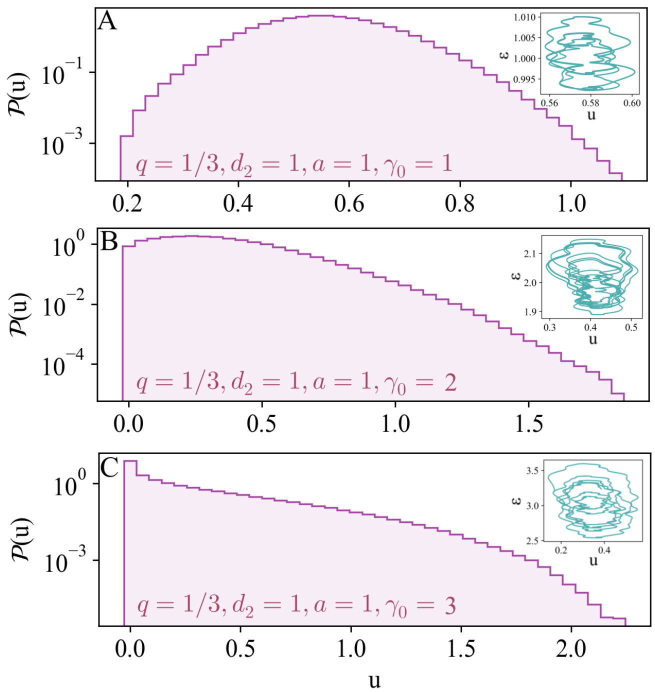

Fig. 6 In the limit of strong frictional forces, the distribution becomes skew (A) before becoming monotonic (B, C). Insets show a single particle phase-space trajectory. Parameters indicated in figure.

5 Discussion

To summarize, we considered the dynamics of non-interacting active particles with internal energy depot and submersed in quenched disordered landscapes. We show that in the fast-relaxation approximation an equation of motion for the mean square displacement can be derived, from which temporal scaling can be extracted. For a power-law medium, the predicted anomalous diffusion exponent agrees well with numerical findings and is similar to that of passive Brownian motion.

In the case of a disordered landscape, the internal energy and self-propulsion speed displays irregular behavior where the phase-space trajectories are seemingly random. Distributions of self-propulsion speeds are studied numerically in the case of deterministic dynamics, so to extract only the distribution resulting from the landscape. In the regime of a small disorder strength the simulations show that the self-propulsion speed distribution is Gaussian with a standard deviation that increases linearly with disorder strength. For stronger disorder the distribution becomes more skew, such that, in the limit of very strong friction, the distributions become monotonically decreasing.

In future studies, several natural extensions could be investigated. Collective effects are not included, and both steric and alignment interactions could display anomalous behaviors when compared to motion in homogeneous environments. Realistic environments will typically have both frictional disorder, or alternatively hard obstacles, in addition to spatially inhomogeneously distributed nutrients. Such systems could be treated similarly as here, while in these cases chemotaxis is likely play an important role.

Conflicts of interest

There are no conflicts to declare.

Acknowledgements

This work was supported by the Research Council of Norway through the Center of Excellence funding scheme, Project No. 262644(PoreLab). L.A. acknowledges support from the Kavli Institute for Theoretical Physics through the National Science Foundation under Grant No. NSF PHY-1748958.

Notes and references

1 M. C. Marchetti, J.-F. Joanny, S. Ramaswamy, T. B. Liverpool, J. Prost, M. Rao and R. A. Simha, *Reviews of Modern Physics*, 2013, **85**, 1143.
2 M. Bär, R. Großmann, S. Heidenreich and F. Peruani, *Annual Review of Condensed Matter Physics*, 2020, **11**, 441–466.
3 P. Isermann and J. Lammerding, *Nucleus*, 2017, **8**, 268–274.
4 J. Gannon, U. Mingelgrin, M. Alexander and R. Wagenet, *Soil Biology and Biochemistry*, 1991, **23**, 1155–1160.
5 W. Y. Wang, C. D. Davidson, D. Lin and B. M. Baker, *Nature communications*, 2019, **10**, 1–12.
6 R. D. Sochol, A. T. Higa, R. R. Janairo, S. Li and L. Lin, *Soft Matter*, 2011, **7**, 4606–4609.
7 J. Park, D.-H. Kim and A. Levchenko, *Biophysical journal*, 2018, **114**, 1257–1263.
8 L. Pieuchot, J. Marteau, A. Guignandon, T. Dos Santos, I. Brigaud, P.-F. Chauvy, T. Cloatre, A. Ponche, T. Petithory, P. Rougerie *et al.*, *Nature communications*, 2018, **9**, 1–13.
9 R. Alonso-Matilla, B. Chakrabarti and D. Saintillan, *Physical Review Fluids*, 2019, **4**, 043101.
10 P. Aceves-Sanchez, P. Degond, E. E. Keaveny, A. Manhart, S. Merino-Aceituno and D. Peurichard, *arXiv preprint arXiv:2004.12638*, 2020.
11 A. M. Ketner, R. Kumar, T. S. Davies, P. W. Elder and S. R. Raghavan, *Journal of the American Chemical Society*, 2007, **129**, 1553–1559.
12 P. Romanczuk, M. Bär, W. Ebeling, B. Lindner and L. Schimansky-Geier, *The European Physical Journal Special Topics*, 2012, **202**, 1–162.

13 A. P. Solon, M. E. Cates and J. Tailleur, *The European Physical Journal Special Topics*, 2015, **224**, 1231–1262.

14 F. Peruani and I. S. Aranson, *Physical Review Letters*, 2018, **120**, 238101.

15 C. Sándor, A. Libál, C. Reichhardt and C. J. Olson Reichhardt, *Phys. Rev. E*, 2017, **95**, 032606.

16 M. A. Fernandez-Rodriguez, F. Grillo, L. Alvarez, M. Rathlef, I. Buttinoni, G. Volpe and L. Isa, *Nature communications*, 2020, **11**, 1–10.

17 C. Datt and G. J. Elfring, *Physical Review Letters*, 2019, **123**, 158006.

18 W. Ebeling, F. Schweitzer and B. Tilch, *BioSystems*, 1999, **49**, 17–29.

19 F. Schweitzer, W. Ebeling and B. Tilch, *Physical Review Letters*, 1998, **80**, 5044.

20 B. O'Shaughnessy and I. Procaccia, *Phys. Rev. Lett.*, 1985, **54**, 455–458.

21 K. S. Olsen, E. G. Flekkøy, L. Angheluta, J. M. Campbell, K. J. Måløy and B. Sandnes, *New Journal of Physics*, 2019.

22 K. S. Olsen and J. M. Campbell, *Frontiers in Physics*, 2020, **8**, 83.

23 M. Burgis, V. Schaller, M. Glässl, B. Kaiser, W. Köhler, A. Krekhov and W. Zimmermann, *New Journal of Physics*, 2011, **13**, 043031.

Notes and references

1 M. C. Marchetti, J.-F. Joanny, S. Ramaswamy, T. B. Liverpool, J. Prost, M. Rao and R. A. Simha, *Reviews of Modern Physics*, 2013, **85**, 1143.

2 M. Bär, R. Großmann, S. Heidenreich and F. Peruani, *Annual Review of Condensed Matter Physics*, 2020, **11**, 441–466.

3 P. Isermann and J. Lammerding, *Nucleus*, 2017, **8**, 268–274.

4 J. Gannon, U. Mingelgrin, M. Alexander and R. Wagenet, *Soil Biology and Biochemistry*, 1991, **23**, 1155–1160.

5 W. Y. Wang, C. D. Davidson, D. Lin and B. M. Baker, *Nature communications*, 2019, **10**, 1–12.

6 R. D. Sochol, A. T. Higa, R. R. Janairo, S. Li and L. Lin, *Soft Matter*, 2011, **7**, 4606–4609.

7 J. Park, D.-H. Kim and A. Levchenko, *Biophysical journal*, 2018, **114**, 1257–1263.

8 L. Pieuchot, J. Marteau, A. Guignandon, T. Dos Santos, I. Brigaud, P.-F. Chauvy, T. Cloatre, A. Ponche, T. Petithory, P. Rougerie *et al.*, *Nature communications*, 2018, **9**, 1–13.

9 R. Alonso-Matilla, B. Chakrabarti and D. Saintillan, *Physical Review Fluids*, 2019, **4**, 043101.

10 P. Aceves-Sanchez, P. Degond, E. E. Keaveny, A. Manhart, S. Merino-Aceituno and D. Peurichard, *arXiv preprint arXiv:2004.12638*, 2020.

11 A. M. Ketner, R. Kumar, T. S. Davies, P. W. Elder and S. R. Raghavan, *Journal of the American Chemical Society*, 2007, **129**, 1553–1559.

12 P. Romanczuk, M. Bär, W. Ebeling, B. Lindner and L. Schimansky-Geier, *The European Physical Journal Special Topics*, 2012, **202**, 1–162.

13 A. P. Solon, M. E. Cates and J. Tailleur, *The European Physical Journal Special Topics*, 2015, **224**, 1231–1262.

14 F. Peruani and I. S. Aranson, *Physical Review Letters*, 2018, **120**, 238101.

15 C. Sándor, A. Libál, C. Reichhardt and C. J. Olson Reichhardt, *Phys. Rev. E*, 2017, **95**, 032606.

16 M. A. Fernandez-Rodriguez, F. Grillo, L. Alvarez, M. Rathlef, I. Buttinoni, G. Volpe and L. Isa, *Nature communications*, 2020, **11**, 1–10.

17 C. Datt and G. J. Elfring, *Physical Review Letters*, 2019, **123**, 158006.

18 W. Ebeling, F. Schweitzer and B. Tilch, *BioSystems*, 1999, **49**, 17–29.

19 F. Schweitzer, W. Ebeling and B. Tilch, *Physical Review Letters*, 1998, **80**, 5044.

20 B. O'Shaughnessy and I. Procaccia, *Phys. Rev. Lett.*, 1985, **54**, 455–458.

21 K. S. Olsen, E. G. Flekkøy, L. Angheluta, J. M. Campbell, K. J. Måløy and B. Sandnes, *New Journal of Physics*, 2019.

22 K. S. Olsen and J. M. Campbell, *Frontiers in Physics*, 2020, **8**, 83.

23 M. Burgis, V. Schaller, M. Glässl, B. Kaiser, W. Köhler, A. Krekhov and W. Zimmermann, *New Journal of Physics*, 2011, **13**, 043031.

Table of contents entry for article "Active particles moving through disordered landscapes":

"The dynamical behavior of active particles moving through a landscape with spatially dependent friction coefficient is investigated analytically and numerically. A fast-relaxation regime and a strongly disordered regime are studied."

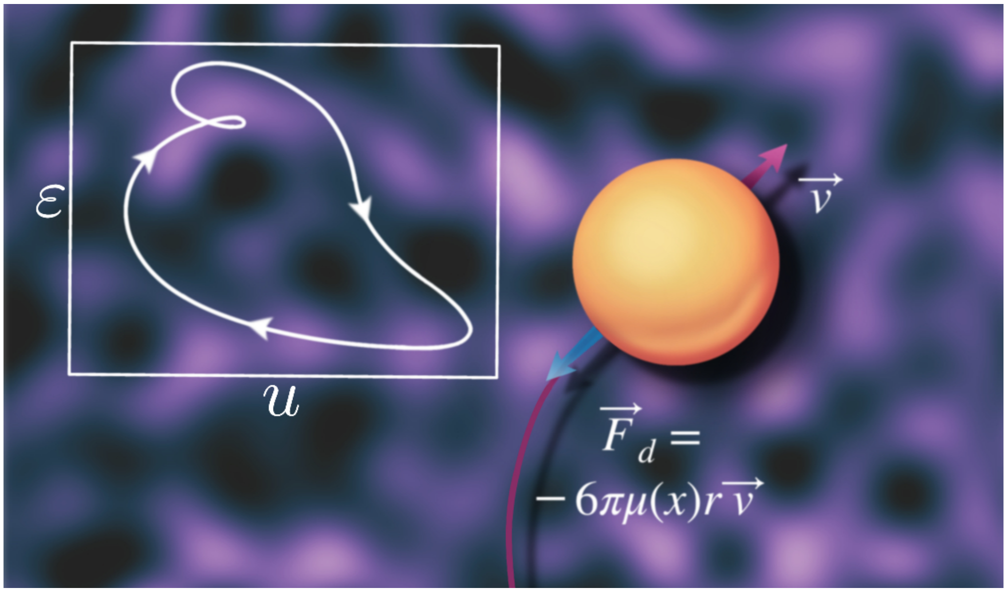
ε
u
$\vec{v}$
$\vec{F}_d =$
$-6\pi\mu(x)r\vec{v}$